

ebony* affects pigmentation divergence and cuticular hydrocarbons in *Drosophila americana* and *D. novamexicana

1 **Abigail M. Lamb¹, Zinan Wang^{2,3}, Patricia Simmer¹, Henry Chung^{2,3}, and Patricia J.**
2 **Wittkopp^{*1,4}**

3 ¹Department of Molecular, Cellular, and Developmental Biology, University of Michigan, Ann
4 Arbor, MI, United States

5 ²Department of Entomology, Michigan State University, East Lansing, MI, United States

6 ³Ecology, Evolutionary Biology, and Behavior Program, Michigan State University, East Lansing,
7 MI, United States

8 ⁴Department of Ecology and Evolutionary Biology, and Behavior Program, University of Michigan,
9 Ann Arbor, MI, United States

10

11 *** Correspondence:**

12 Patricia J Wittkopp

13 wittkopp@umich.edu

14 **Keywords: CRISPR, Cas9, melanin, nanos, abdominal pigmentation, genome editing, virilis**
15 **group**

16 **1 Abstract**

17 *Drosophila* pigmentation has been a fruitful model system for understanding the genetic and
18 developmental mechanisms underlying phenotypic evolution. For example, prior work has shown
19 that divergence of the *tan* gene contributes to pigmentation differences between two members of the
20 virilis group: *Drosophila novamexicana*, which has a light yellow body color, and *D. americana*,
21 which has a dark brown body color. Quantitative trait locus (QTL) mapping and expression analysis
22 has suggested that divergence of the *ebony* gene might also contribute to pigmentation differences
23 between these two species. Here, we directly test this hypothesis by using CRISPR/Cas9 genome
24 editing to generate *ebony* null mutants in *D. americana* and *D. novamexicana* and then using
25 reciprocal hemizyosity testing to compare the effects of each species' *ebony* allele on pigmentation.
26 We find that divergence of *ebony* does indeed contribute to the pigmentation divergence between
27 species, with effects on both the overall body color as well as a difference in pigmentation along the
28 dorsal abdominal midline. Motivated by recent work in *D. melanogaster*, we also used the *ebony* null
29 mutants to test for effects of *ebony* on cuticular hydrocarbon (CHC) profiles. We found that *ebony*
30 affects CHC abundance in both species, but does not contribute to qualitative differences in the CHC
31 profiles between these two species. Additional transgenic resources for working with *D. americana*
32 and *D. novamexicana*, such as *white* mutants of both species and *yellow* mutants in *D. novamexicana*,
33 were generated in the course of this work and are also described. Taken together, this study advances
34 our understanding of loci contributing to phenotypic divergence and illustrates how the latest genome
35 editing tools can be used for functional testing in non-model species.

36

37 2 Introduction

38 Insect pigmentation is a well-studied trait that displays a variety of phenotypic differences within and
39 between species (Kronforst et al. 2012; Wittkopp et al. 2003). These differences have evolved over a
40 wide range of divergence times and in a great diversity of ecological contexts. Differences in insect
41 pigmentation often appear to be ecologically relevant, correlating with geographic and climatic
42 factors and playing a role in phenomena such as mate recognition, camouflage, thermoregulation, and
43 water balance (True 2003; Wittkopp and Beldade 2009). Studies of pigmentation differences within
44 the genus *Drosophila* have emerged as a productive model for studying the evolution of
45 development, exploiting the diversity of phenotypes as well as genetic tools available for working
46 with *Drosophila* and a long history of research into the genetic and biochemical mechanisms
47 controlling pigmentation development (Wittkopp et al. 2003; Massey and Wittkopp 2016; Rebeiz and
48 Williams 2017). Indeed, since the early 2000s, the genetic bases of dozens of pigmentation
49 differences have been identified in varying levels of detail. Strikingly, in every case where a causal
50 role has been directly attributed to a specific gene, the mechanism of change has been found to be a
51 *cis*-regulatory change that affects gene expression rather than a change in the protein's function
52 (Massey and Wittkopp 2016). These case studies have also identified multiple independent instances
53 of divergent expression for some pigmentation genes, suggesting that these genes are particularly
54 tractable routes for the evolution of pigmentation in this genus (Massey and Wittkopp 2016).

55 Changes in *cis*-regulatory sequences are thought to be a common mechanism of developmental
56 evolution because they tend to be less pleiotropic than changes in protein function (Wray et al. 2003;
57 Carroll 2005). For example, a *cis*-regulatory change might alter a gene's expression in only a single
58 tissue or a single point in development whereas changing its protein function is expected to impact
59 the organism everywhere that protein is expressed. Genes controlling pigmentation development in
60 *Drosophila* might be especially likely to evolve using this mechanism because the proteins encoded
61 by these genes are also required for other biological functions. For example, genes required for
62 pigment synthesis have also been shown to affect mating success, circadian rhythm, vision, and
63 innate immunity (Massey et al. 2019a; Suh and Jackson 2007; True et al. 2005; Nappi and
64 Christensen 2005; Takahashi 2013; Wittkopp and Beldade 2009). The pigmentation biosynthesis
65 genes *ebony* and *tan* have also been found to affect the profiles of cuticular hydrocarbons on adult
66 flies, which are hydrophobic lipids on the surface of insect cuticle that are involved in chemical
67 communication, mate recognition, and water balance (Massey et al. 2019b; Chung and Carroll 2015;
68 Chung et al. 2014).

69 Here, we investigate genetic changes contributing to the evolution of novel body color in *D.*
70 *novamexicana*. This species has evolved a much lighter and more yellow body color than its sister
71 species *D. americana* during the approximately 400,000 years since these species diverged from their
72 most recent common ancestor (Figure 1, Caletka and McAllister 2004; Morales-Hojas et al. 2008). *D.*
73 *novamexicana* and *D. americana* show signs of reproductive isolation (Ahmed-Braimah and
74 McAllister 2012; Patterson and Stone 1949), but they are interfertile and can produce viable, fertile
75 F₁ hybrids in the laboratory, allowing genetic analysis (Wittkopp et al. 2003; Wittkopp et al. 2009).
76 Prior genetic mapping has identified two quantitative trait loci (QTL) that together account for ~87%
77 of the pigmentation difference between *D. novamexicana* and *D. americana* (Wittkopp et al. 2009).
78 Fine mapping and transgenic analysis revealed that the QTL of smaller effect was driven by
79 divergence at *tan* (Wittkopp et al. 2009), a gene that encodes a hydrolase that catalyzes the
80 conversion of N-B-alanyl dopamine (NBAD) to dopamine, a precursor for dark melanin pigment
81 (True et al. 2005). The QTL of larger effect was linked to an inverted region containing the candidate
82 gene *ebony*, but the presence of the inversion prevented fine mapping to separate the effects of *ebony*

83 from linked loci (Wittkopp et al. 2009). *ebony* encodes a synthetase that catalyzes the conversion of
84 dopamine into NBAD, a precursor for light yellow pigments (Koch et al. 2000), which is the opposite
85 of the reaction catalyzed by Tan. *ebony* has also been shown to have expression differences between
86 *D. novamexicana* and *D. americana* caused by *cis*-regulatory divergence (Cooley et al. 2012).

87 Despite these data suggesting that *ebony* contributes to pigmentation divergence between *D.*
88 *novamexicana* and *D. americana*, the phenotypic effects of sequence divergence at *ebony* have not
89 been demonstrated. Here, we show that divergence at *ebony* does indeed contribute to pigmentation
90 divergence between these two species. We use CRISPR/Cas9 genome editing to mutate *ebony* in
91 both species and use these mutant genotypes to directly test *ebony*'s contribution to pigmentation
92 divergence through reciprocal hemizygoty testing (Stern 2014). We find that the *D. novamexicana*
93 *ebony* allele causes lighter pigmentation throughout the body than the *D. americana* *ebony* allele. We
94 also find that allelic divergence at *ebony* is primarily responsible for a spatial difference in abdominal
95 pigmentation between these species: the *D. novamexicana* *ebony* allele causes the absence of dark
96 melanin along the dorsal midline of the abdomen seen in *D. novamexicana*. Finally, we show that
97 *ebony* affects the cuticular hydrocarbon (CHC) profiles in *D. americana* and *D. novamexicana*, but
98 does not contribute to the qualitative differences in CHC profiles seen between species. Taken
99 together, our data show the power of using CRISPR/Cas9 genome editing to test functional
100 hypotheses about evolutionary mechanisms. In addition, resources generated and lessons learned in
101 the course of this work are expected to help other researchers perform CRISPR/Cas9 genome editing
102 in *D. americana*, *D. novamexicana* and other *Drosophila* species.

103 3 Materials and Methods

104 3.1 Fly stocks and husbandry

105 The following fly lines were used in this study: *D. americana* "A00" (National *Drosophila* Species
106 Stock Center number 15010-0951.00), *D. novamexicana* "N14" (National *Drosophila* Species Stock
107 Center number 15010-1031.14), *D. lummei* (National *Drosophila* Species Stock Center number
108 15010-1011.08), *D. virilis* (National *Drosophila* Species Stock Center number 15010-1051.87), *D.*
109 *melanogaster* $y^1 M\{w[+mC]=nos-Cas9.P\}ZH-2A w^*$ (Bloomington *Drosophila* Stock Center number
110 54591), and *D. melanogaster* Canton-S. All flies were reared on standard cornmeal medium at 23-
111 25°C with a 12:12 hour light:dark cycle.

112 3.2 Transgenesis and CRISPR mutant generation in *D. americana* and *D. novamexicana*

113 To the best of our knowledge, prior to this work, the only transformation of *D. americana* or *D.*
114 *novamexicana* resulted from the insertion of a piggyBac transgene (Wittkopp et al. 2009). We
115 therefore first used the CRISPR/Cas9 system to generate *white* mutants in both species to test the
116 feasibility of CRISPR genome modification and to create lines that are easier to screen for common
117 transformation markers that drive expression of fluorescent proteins or restore red pigmentation in
118 the eyes by restoring *white* function. We successfully generated *white* mutant N14 and A00 lines
119 used as transgenic hosts for future work, by injecting single guide RNAs (sgRNAs) targeting coding
120 sequences in *white* conserved between *D. novamexicana* and *D. americana* in the second and third
121 exons and screening for the loss of red eye pigment in male offspring of injected females
122 (Supplementary Figure 1); *white* is on the X chromosome and thus only present in a single copy in
123 males. These same guide RNAs were also used in *Drosophila virilis* to cut *white* and integrate an attP
124 landing site potentially useful for site-directed transgene insertion (J. Lachoweic and P.J. Wittkopp,
125 unpublished data), although the PhiC31 system does not seem to work well in *D. virilis* (Stern et al.
126 2017). For all CRISPR experiments, sgRNAs were in-vitro transcribed from DNA templates using

127 Invitrogen T7 MEGAscript Transcription Kit according to protocol described by Bassett et al. 2013.
128 Oligonucleotides used to generate sgRNAs are listed in Supplementary Table 1. After transcription,
129 sgRNAs were purified using RNA Clean and Concentrator 5 kit (Zymo Research), eluted with
130 nuclease-free water, and quantified with Qubit RNA BR Assay Kit (Thermo Fisher Scientific). For
131 CRISPR injections, sgRNAs were mixed with purified Cas9 protein (PNA Bio #CP01) with a final
132 injected concentration of 0.05% phenol red to visualize the injection mix. CRISPR injections were
133 performed in-house, using previously described methods (Miller et al. 2002).

134 To try to increase efficiency of CRISPR mutagenesis in these species, we next sought to generate
135 transgenic lines expressing Cas9 in the germlines of *white* mutant *D. americana* (A00) and *D.*
136 *novamexicana* (N14) flies using piggyBac transgenesis (Horn and Wimmer 2000). Based on prior
137 reports that the *nanos* (*nos*) promoter and 3'UTR drive expression in the germline of *Drosophila*
138 *virilis* (Holtzman et al. 2010), a close relative of *D. americana* and *D. novamexicana*, we amplified
139 the *nos-Cas9-nos* transgene from the *pnos-Cas9-nos* plasmid (Addgene #62208; Port et al. 2014)
140 using Phusion High Fidelity Polymerase (NEB) with tailed primers and cloned the amplicon into
141 pBac{3XP3-ECFPafm} (Horn and Wimmer 2000) digested with AscI and Bsu36I restriction
142 enzymes using Gibson Assembly Master Mix (NEB). Primers are included in Supplemental Table 1.
143 We confirmed the insert was correctly incorporated and free of PCR-induced errors by Sanger
144 sequencing. We sent the *white* mutant lines of *D. americana* A00 and *D. novamexicana* N14 that we
145 generated to Rainbow transgenic services for piggyBac transgenesis (www.rainbowgene.com) and
146 screened offspring of injected adults for expression of the enhanced cyan fluorescent protein (ECFP)
147 in the eye using a Leica MZ6 stereoscope equipped with a Kramer Scientific Quad Fluorescence
148 Illuminator. Transformants were obtained from injections into *D. novamexicana* (N14) (PCR
149 verified), but not from injections into *D. americana* (A00), despite multiple attempts.

150 All subsequent CRISPR injections in *D. novamexicana* were performed using flies homozygous for
151 the *nos-Cas9-nos* transgene, some with and some without the inclusion of commercially available
152 Cas9 protein in the injection mix. CRISPR mutants were only obtained from injections containing the
153 commercially available Cas9 protein, however, suggesting that the *nos-Cas9-nos* transgene might not
154 drive expression of Cas9 in the germline of *D. novamexicana*. To test this hypothesis, we used
155 western blotting to examine Cas9 protein expression in 3 transformed *D. novamexicana* N14 lines
156 with independent insertions of the piggyBac transgene and in a *D. melanogaster* transgenic line
157 carrying the original *pnos-Cas9-nos* transgene (Bloomington Drosophila Stock Center line 54591,
158 transformed with Addgene plasmid #62208, Port et al. 2014). These experiments showed that the
159 *nos-Cas9-nos* transgene in *D. novamexicana* N14 flies does not express Cas9 protein in the ovaries
160 (Supplementary Figure 2). This conclusion was further supported when injection of sgRNAs
161 targeting the *yellow* gene into the *D. novamexicana* line carrying the *nos-Cas9-nos* transgene also
162 only produced *yellow* mutants when the Cas9 protein was co-injected with the sgRNAs
163 (Supplementary Figure 3). Ability of the *nos* promoter to drive germline expression in the closely
164 related species *D. virilis* has also been found to be variable among transgenic lines (Hannah
165 McConnell, Aida de la Cruz, and Harmit Malik, personal communication), suggesting that other
166 promoters should be used in the future to drive reliable germline expression in the *virilis* group.

167
168 To generate *ebony* mutant *D. americana* (A00) and *D. novamexicana* (N14), we synthesized five
169 sgRNAs targeting conserved sites in the first coding exon of *ebony*. Because *ebony* is located on an
170 autosome and *ebony* loss-of-function mutant alleles are generally considered recessive in *D.*
171 *melanogaster* (Thurmond et al. 2019), we did not expect to be able to identify *ebony* mutants by
172 simply screening progeny of injected flies for mutant phenotypes as we did for *white* and *yellow*. We
173 therefore co-injected a donor plasmid containing the sequence of an eye-specific red fluorescent

174 protein marker (3XP3-RFP) flanked by *ebony* sequences that could be inserted into *ebony* via
175 homology-directed repair and used to screen for *ebony* mutants. Although we observed RFP
176 expression in larvae injected with the homology-directed repair donor fragment, indicating that the
177 reporter gene was functional in these species, injected individuals did not produce any offspring with
178 red fluorescent eyes, suggesting that the donor plasmid was not integrated in the germline of injected
179 individuals. Because non-homologous end joining occurs more frequently than homology directed
180 repair following double-strand breaks (Liu et al. 2018), we also tried to identify flies that might be
181 heterozygous for an *ebony* mutant allele by closely inspecting all offspring of injected (G_0) flies for
182 any subtle changes in pigmentation. Specifically, we collected and mated (G_1) offspring of injected
183 flies with any noticeably darker pigmentation, keeping them grouped by G_0 parent of origin. As
184 further described in the results, we were ultimately able to identify homozygous *ebony* mutants
185 among progeny from these $G_1 \times G_1$ crosses of relatively dark flies derived from two independent *D.*
186 *novamexicana* G_0 flies and one *D. americana* G_0 fly. Sanger sequencing these flies confirmed they
187 were homozygous for *ebony* alleles containing deletions. We then crossed the mutated *ebony* alleles
188 back into wild-type backgrounds of each parental species to generate homozygous *ebony* mutant lines
189 with wild-type red eyes.

190 3.3 Western blotting

191 For *ebony* western blotting, proteins were extracted from stage P14/15 pupae, identified by the
192 following characteristics: black pigmentation present in wings and bristles, meconium visible in
193 abdomen (Cooley et al. 2012). For each sample, five pupae were homogenized in 100uL of
194 homogenization buffer (125 mM Tris pH 6.8, 6% SDS, 2.5X Roche cOMplete protease inhibitor
195 cocktail, EDTA-free), then centrifuged for 15 minutes at 15000rcf, and the supernatant transferred to
196 a fresh tube with an equal volume of 2x Laemmli buffer (125 mM Tris pH 6.8, 6% SDS, 0.2%
197 glycerol, 0.25% bromophenol blue, 5% Beta-mercaptoethanol).

199 For Cas9 western blotting, protein was extracted from ovaries dissected in ice cold PBS from the
200 following lines: untransformed N14 *white* mutants (host line), three independently transformed lines
201 of N14 *white* carrying the pBac{3XP3-ECFPafm-nosCas9nos} transgene, transgenic *D.*
202 *melanogaster* carrying the *pnos-Cas9-nos* transgene, and wild-type (Canton-S) *D. melanogaster*. For
203 *D. novamexicana* samples, we collected ovaries from 10 sexually mature flies, whereas for *D.*
204 *melanogaster* samples, we collected ovaries from 18 sexually mature flies. Different numbers of flies
205 were used for the two species because of differences in body size. In each case, ovaries were placed
206 into microcentrifuge tubes on ice, spun down briefly in a tabletop centrifuge, and excess PBS was
207 removed and replaced with 20uL of homogenization buffer. Samples were then treated as described
208 for *ebony* western blots above. A positive control Cas9 sample was made by diluting purified Cas9
209 protein (PNA Bio CP01) in homogenization buffer, and mixing with 2X Laemmli buffer to a final
210 concentration of 2.5ng/uL.

211
212 Samples were heated at 95°C for 10 minutes before loading into 7.5% Mini-PROTEAN® TGX™
213 Precast Protein Gels (BioRad) and running at 150V for approximately 90 minutes at 4°C in 1X tris-
214 glycine running buffer. Separate gels were run for *ebony* and Cas9 blots. Samples were loaded in the
215 following volumes: 35uL per pupa sample, 30uL per ovary sample, 10uL of Cas9 positive control
216 (25ng protein), 5uL PageRuler prestained protein ladder (Thermo Scientific). Gels were transferred
217 onto PVDF membrane in tris-glycine transfer buffer, 10% MeOH, 0.01% SDS at 100V for 1 hour
218 with stirring on ice at 4°C. Membranes were blocked in 3% nonfat dry milk in TBST for 30 minutes
219 at RT with shaking, then divided in half using the prestained ladder as a guide just below the 100kDa
220 mark for the Cas9 membrane and just below the 70kDa mark for the *ebony* membrane. The lower

221 molecular weight halves of the membranes were placed in solutions containing primary antibodies to
222 detect the protein used as a loading control (tubulin or lamin), whereas the halves of the membranes
223 containing the higher molecular weight proteins were placed in solutions containing primary
224 antibody solutions against the protein of interest (*Ebony* or Cas9), each diluted in 3% nonfat dry milk
225 in TBST. In all cases, membranes were incubated with the primary antibodies overnight at 4°C.
226 Primary antibody solutions for *ebony* included rabbit anti-*ebony* 1:300 (Wittkopp et al. 2002) and
227 rabbit anti-alpha tubulin 1:5000 (Abcam ab52866) as a loading control. Primary antibody solutions
228 for Cas9 included mouse anti-Cas9 1:1000 (Novus NBP2-36440) and mouse anti-lamin 1:200
229 (DHSB adl67.10) as a loading control. Membranes were washed in TBST and transferred to
230 secondary antibody solutions diluted in 3% nonfat milk in TBST for 2 hours at RT. The following
231 secondary antibodies were used: donkey anti-rabbit HRP 1:5000 (Amersham na934) or goat anti-
232 mouse HRP 1:5000 (abcam ab97023). Membranes were finally washed in TBST and developed with
233 SuperSignal West Pico Chemiluminescent Substrate (Thermo Scientific) and imaged using a Licor
234 Odyssey FC imaging system.

235 **3.4 Fly crosses for reciprocal hemizyosity testing and cuticular hydrocarbon analysis**

236 To generate F₁ hybrids carrying only one (*D. americana* or *D. novamexicana*) functional *ebony*
237 allele, wild-type and *ebony* mutant flies from each species were collected as virgins and aged in vials
238 for at least 12 days to reach sexual maturity and verify virgin female status by absence of larvae.
239 Crosses were all set on the same batch of food on the same day and placed at 25°C. For most crosses,
240 4 virgin females and 4 males were used; however, 8 virgin females and 8 males were used in
241 interspecific crosses with *D. novamexicana* females because of reduced mating success in these
242 crosses. After 3 days, adult flies from these crosses that would be used for cuticular hydrocarbon
243 (CHC) analysis were transferred to new vials with a fresh batch of food. Offspring from the first set
244 of vials were used for imaging and pigmentation analysis, while offspring from the second set of
245 vials were used for CHC analysis. Flies used for pigmentation phenotyping were aged 5-7 days after
246 eclosion and preserved in 10% glycerol in ethanol before imaging (Wittkopp et al. 2011).

247 **3.5 Imaging of fly phenotypes**

248 Insect specimens were imaged using a Leica DC480 camera attached to a Leica MZ16F stereoscope
249 equipped with a ring light attachment and Leica KL 1500 LCD lamp. Images were captured using
250 Leica DC Twain software version 5.1.1 run through Adobe Photoshop CS6 version 13.0 X32. Prior
251 to imaging, pupal cases and wings were mounted on slides in PVA mounting medium (BioQuip).
252 Thorax, abdomen, and whole-body specimens were prepared from age-matched, preserved flies as
253 described in the previous section. For imaging, thorax, abdomen, and whole-body specimens were
254 submerged in 100% ethanol in custom wells composed of white oven-cured polymer clay (Sculpey).
255

256 Because the color of specimens spanned a wide range across genotypes, exposure was optimized for
257 each sample type (e.g. whole body, thorax, abdomen, wing, pupal case) individually by placing
258 specimens from the two phenotypic extremes in the same frame and adjusting exposure to avoid
259 over-exposing the lightest flies while capturing as much detail as possible from the darkest flies.
260 Exposure time, lighting, white balance, background, and zoom were kept identical across all images
261 of single tissue type. Minor color adjustments to improve visibility of phenotypes were performed
262 simultaneously across all raw images of the same sample type in a single combined document using
263 Photoshop CC 2019, ensuring that all images presented for direct comparisons were adjusted
264 identically.

265 **3.6 Cuticular hydrocarbon analyses**

266 CHCs for each cross were extracted from five 5-day-old females by soaking the flies for 10 mins in
267 200 μ l hexane containing hexacosane (C26; 25 ng/ μ l) as an internal standard. Eight replicates were
268 prepared for each cross. Extracts were directly analyzed by the GC/MS (7890A, Agilent
269 Technologies Inc., Santa Clara, CA) coupled with a DB-17ht column 30 m by 0.25 mm (i.d.) with a
270 0.15 μ m film thickness (Agilent Technologies Inc., Santa Clara, CA). Mass spectra were acquired in
271 Electron Ionization (EI) mode (70 eV) with Total Ion Mode (TIM) using the GC/MS (5975C, Agilent
272 Technologies Inc., Santa Clara, CA). The peak areas were recorded by MassHunter software (Agilent
273 Technologies Inc., Santa Clara, CA). Helium was the carrier gas at 0.7 ml/min and the GC thermal
274 program was set as follows: 100 $^{\circ}$ C for 4 min, 3 $^{\circ}$ C/min to 325 $^{\circ}$ C. Straight-chain compounds were
275 identified by comparing retention times and mass spectra with authentic standard mixture (C6-C40)
276 (Supelco[®] 49452-U, Sigma-Aldrich, St. Louis, MO). Methyl-branched alkanes, alkenes, dienes and
277 trienes were then identified by a combination of their specific fragment ions on the side of functional
278 groups (methyl branch or double bonds) and retention times relative to linear-chain hydrocarbon
279 standards. Each individual CHC peak was quantified by normalizing its peak area to the peak area of
280 the internal C26 standard, converting each CHC peak area to ng/fly using the known internal
281 standard concentration of 1000 ng/fly. Welch's *t*-tests with a Benjamini-Hochberg correction for
282 multiple testing (Benjamini and Hochberg 1995) were used to compare CHC amounts between pairs
283 of genotypes. To compare the effects of *ebony* loss of function on different chain-lengths of CHCs,
284 eight biological replicates of homozygous *ebony* null measurements were divided by the mean
285 measurement of the eight replicates of the matched *ebony* heterozygote for each individual CHC. The
286 ratio of *ebony* null to heterozygote CHC abundance was plotted against CHC chain length. The
287 relative effects of *D. americana* versus *D. novamexicana* *ebony* in a common F₁ hybrid background
288 (described as F₁[*e^A/e*] and F₁[*e^N/e*], respectively) were also compared in this manner, with the
289 replicates of the F₁[*e^A/e*] divided by the mean F₁[*e^N/e*] measurement for each CHC. We used
290 Spearman's rank correlation (Spearman's rho) to test the relationship between CHC chain length and
291 the effect of *ebony* on CHC abundance. The threshold for statistical significance was set at *alpha* =
292 0.05 for all tests. Datafile and R code used for this analysis are provided in Supplementary Files 1
293 and 2, respectively

294 4 Results and Discussion

295

296 The reciprocal hemizyosity test is a powerful strategy for identifying genes with functional
297 differences that contribute to phenotypic divergence (reviewed in Stern 2014). This test is performed
298 by comparing the phenotypes of two hybrid genotypes that are genetically identical except for which
299 allele of the candidate gene is mutated. Any phenotypic differences observed between these two
300 genotypes are attributed to divergence of the candidate gene. Applying this test to identify functional
301 differences between species requires loss-of-function (null) mutant alleles in both species and the
302 ability for the species to cross and produce F₁ hybrids. Consequently, in order to use this strategy to
303 test *ebony* for functional divergence between *D. novamexicana* and *D. americana*, we first needed to
304 generate *ebony* null mutant alleles in both species.
305

306 4.1 Generating *ebony* mutants in *D. americana* and *D. novamexicana* using CRISPR/Cas9

307

308 We generated *ebony* null mutants in *D. novamexicana* and *D. americana* by using CRISPR/Cas9 to
309 target double-strand breaks to five conserved sites within the first coding exon of *ebony*. As
310 described more fully in the Methods section, we injected embryos of *white* mutants from both species
311 with purified Cas9 protein and sgRNAs targeting all five sites simultaneously. To make it easier to

312 identify *ebony* mutant alleles, we also injected a donor plasmid that would allow homology directed
313 repair to integrate a transgene expressing red fluorescent protein in the fly's eyes, but no progeny of
314 injected flies were observed to express this transformation marker. We reasoned that *ebony* mutants
315 might still have been generated by non-homologous end-joining, however, and thus also searched for
316 *ebony* mutants by looking for changes in body pigmentation.

317
318 In *D. melanogaster*, *ebony* loss-of-function mutants have a much darker appearance than wild-type
319 flies because they are unable to produce yellow sclerotin, causing an increase in production of black
320 and brown melanins (Wittkopp et al. 2002). *D. melanogaster ebony* mutant alleles are commonly
321 described as recessive to wild-type *ebony* alleles (Thurmond et al. 2019); however, in some genetic
322 backgrounds, flies heterozygous for an *ebony* mutant allele are slightly darker than wild-type flies
323 (Thurmond et al. 2019). Because *D. novamexicana* has such a light yellow body color (Figure 2A),
324 we thought it possible that flies heterozygous for an *ebony* mutant allele might also show a detectable
325 darkening of pigmentation; we were less optimistic about being able to detect heterozygous *ebony*
326 mutants based on pigmentation in *D. americana* because its wild-type pigmentation is already very
327 dark (Figure 2C). Nonetheless, we sorted through the progeny of injected *D. novamexicana* and *D.*
328 *americana* flies, isolating any individuals that seemed to have darker pigmentation than their siblings
329 and allowing these relatively dark flies to freely mate in vials segregated by injected parents, keeping
330 individual "founder" mutations separate.

331
332 Two of the vials of darker pigmented *D. novamexicana* flies produced pupae with an unusual black
333 pattern on the anterior end of the pupal case (Figure 2J). We moved these pupae to new vials and
334 found that they developed into adults with the much darker than wild-type body color expected for
335 homozygous *ebony* mutants in *D. novamexicana* (Figure 2 A,B). Because pigmentation of the pupal
336 case is very similar between *D. novamexicana* and *D. americana* (Figure 2I,K, Ahmed-Braimah and
337 Sweigart 2015), we also searched for pupae with similar pigmentation marks in the vials containing
338 progeny of darker flies descended from injected *D. americana*. We found such pupae in one of the
339 vials (Figure 2L). Flies emerging from these pupal cases also showed darker pigmentation than wild-
340 type *D. americana* (Figure 2C,D), as expected for homozygous *ebony* mutants, but this difference
341 was much more subtle than in *D. novamexicana* (Figure 2A,B). Flies from both species emerging
342 from pupal cases with abnormal pigmentation also showed increased levels of dark melanins in
343 wings in a pattern similar to that seen in *D. melanogaster ebony* mutants (Figure 2E-H, Wittkopp et
344 al. 2002), further suggesting that they were homozygous for *ebony* mutant alleles. Crossing putative
345 homozygous *ebony* mutants from the same species to each other resulted in true-breeding lines of *D.*
346 *americana* and *D. novamexicana* presumed to be homozygous for *ebony* mutant alleles.

347
348 To determine whether these true-breeding lines were indeed homozygous for *ebony* mutant alleles,
349 we used Sanger sequencing to search for changes in the *ebony* sequence in the region targeted for
350 double strand breaks with CRISPR/Cas9. We found that the presumed *ebony* mutant lines of both
351 species harbored deletions corresponding to the locations of sgRNA target sites in the first coding
352 exon, with the two *D. novamexicana* mutant lines carrying deletions of 7 and 10 bases and the *D.*
353 *americana* mutant line carrying a deletion of 46 bases (Figure 3A). Each of these mutations is
354 expected to cause frameshifts, leading to multiple early stop codons. Further experiments described
355 in this study using *D. novamexicana ebony* mutants were conducted with the 10 base deletion line,
356 and any further description of *ebony* null *D. novamexicana* refers to this line.

357
358 To further assess whether these mutations caused null alleles, we used western blotting to examine
359 the expression of the Ebony protein during late pupal stages when adult pigmentation is developing
360 and the *ebony* gene is expressed in the developing abdomen (Wittkopp, et al. 2002; Cooley et al.

361 2012). We performed western blots on protein extracts from P14/P15 stage pupae of both wild-type
362 and homozygous *ebony* mutant flies of both *D. americana* and *D. novamexicana* using an antibody
363 against *D. melanogaster ebony* (Wittkopp et al. 2002). This antibody recognizes a 94 kDa protein
364 consistent with the predicted molecular weight of Ebony in pupal protein extracts from wild-type
365 lines of both *Drosophila melanogaster* and *Drosophila biarmipes*, but does not produce a 94kDa
366 band in pupal protein extracts of either *e1* or *In(3R)eAFA ebony* mutant lines of *D. melanogaster*
367 (Wittkopp et al. 2002). Wild-type extracts of both *D. americana* and *D. novamexicana* produced
368 presumptive Ebony bands while extracts from flies homozygous for *ebony* deletions did not produce
369 a 94 kDa band for either species (Figure 3B). The nature of the frameshift deletions as well as the
370 western blot evidence together show that these *ebony* mutations cause null alleles.
371

372 **4.2 *ebony* divergence contributes to body color differences between *D. novamexicana* and *D.*** 373 ***americana***

374 We used the homozygous *ebony* mutant *D. novamexicana* and *D. americana* lines to perform a
375 reciprocal hemizygoty test by crossing *ebony* mutant *D. novamexicana* (e^-/e^-) to wild-type *D.*
376 *americana* (e^A/e^A) and *ebony* mutant *D. americana* (e^-/e^-) to wild-type *D. novamexicana* (e^N/e^N)
377 (Figure 4A). In order to observe the effects of the two species' *ebony* alleles in the presence of each
378 species X chromosome, we conducted sets of reciprocal crosses (i.e., swapping the genotypes of the
379 male and female parents). Female F₁ hybrids from reciprocal crosses are genetically identical except
380 for the parent of origin of their one functional *ebony* allele (e^N or e^A). F₁ hybrid females carrying a
381 functional *D. novamexicana* *ebony* allele (F₁[e^N/e^-]) developed a lighter body color than F₁ hybrid
382 females carrying a functional *D. americana* *ebony* allele (F₁[e^A/e^-]) (Figure 4B,C vs D,E). These data
383 demonstrate for the first time that functional divergence between the *D. novamexicana* and *D.*
384 *americana* *ebony* alleles contributes to divergent body color between these two species.
385
386

387 To determine how *ebony* divergence interacts with divergent loci on the X-chromosome, we also
388 compared the body color of male progeny from these reciprocal crosses. Like the F₁ hybrid females,
389 these F₁ hybrid males differ for the parent of origin for their one functional *ebony* allele (e^A or e^N);
390 however, they also differ for the parent of origin of all X-linked genes. Prior work has shown that
391 divergence on the X-chromosome, particularly divergence in non-coding sequences of the *tan* gene,
392 also contributes to differences in body color between *D. novamexicana* and *D. americana* (Wittkopp
393 et al. 2003; Wittkopp et al. 2009). As expected, we found that body color differed between males
394 carrying alternate species' X chromosomes (Figure 4F vs G and H vs I) as well as between males
395 carrying the same X chromosome but different species' functional *ebony* alleles (Figure 4F vs H and
396 3F vs I). Consistent with prior findings demonstrating that divergence in the QTL containing *ebony*
397 explained more of the difference in pigmentation than divergence at X-linked genes, we found that
398 males with functional *D. americana* *ebony* alleles had the darkest phenotypes, regardless of their X-
399 chromosome genotype (Figure 4F-I).
400

401 **4.3 *ebony* divergence also contributes to a difference in abdominal pigment patterning** 402 **between *D. novamexicana* and *D. americana***

403 Although the divergent overall body color is the most striking difference in pigmentation between *D.*
404 *novamexicana* and *D. americana*, there is also a difference in the distribution of pigments along the
405

406 dorsal midline of the abdomen between these two species (Figure 1). This difference is also visible in
407 individuals of both species heterozygous for an ebony null allele (Figure 4 J-M). Prior work has
408 shown that the absence of dark pigments seen in this region of *D. novamexicana* is dominant in F₁
409 hybrids to the presence of dark pigments seen in this region of *D. americana* (Wittkopp et al. 2003). In
410 addition, genetic mapping of this trait between *D. novamexicana* and *D. virilis* (which has a dark
411 midline region similar to *D. americana*) has shown that the chromosome including *ebony*
412 (chromosome 2) has a large effect on this trait (Spicer 1991). We found that *D. novamexicana* *ebony*
413 mutants showed even pigmentation across the width of each abdominal segment (Figure 2B),
414 demonstrating that *ebony* is required for the development of lighter pigmentation along the dorsal
415 midline in wild-type *D. novamexicana* (Figure 2A). In addition, comparing the pigmentation of this
416 abdominal dorsal midline region between F₁ hybrid flies of both sexes from the reciprocal crosses
417 described above (Figure 4) showed that divergence at *ebony* contributes to this trait difference
418 between *D. novamexicana* and *D. americana*. Specifically, we observed less dark pigments in the
419 dorsal midline region of the abdomen in F₁ hybrid individuals inheriting the wild-type *D.*
420 *novamexicana* *ebony* allele (F₁[*e^N/e⁻*], Figure 4B,C,F,G) than the *D. americana* *ebony* allele (F₁[*e^A/e⁻*
421]) (Figure 4D,E,H,I). Males carrying a functional *D. novamexicana* *ebony* allele (F₁[*e^N/e⁻*]) showed
422 reduced pigmentation in the dorsal midline relative to the lateral regions regardless of the origin of
423 their X chromosome (Figure 4F,G), indicating that divergent loci on the X-chromosome (including
424 *tan*) do not affect the presence of this phenotype.
425

426 4.4 Cuticular hydrocarbon profiles differ between *D. americana* and *D. novamexicana* and 427 are affected by *ebony* expression but not *ebony* divergence

428
429 *ebony* expression was recently found to affect the relative abundance of cuticular hydrocarbons
430 (CHCs) in *D. melanogaster* (Massey et al. 2019b). In addition, variation in *ebony* expression was
431 also shown to correlate with variation in CHC profiles among natural isolates of *D. melanogaster*
432 (Massey, et al. 2019b). To determine whether *ebony* also effects CHC profiles in *D. novamexicana*
433 and *D. americana*, we extracted CHCs from *D. americana* and *D. novamexicana* female homozygous
434 *ebony* mutant flies as well as females heterozygous for the *ebony* mutant allele. We compared
435 heterozygous individuals (rather than wild-type flies) to mutants homozygous for the *ebony* null
436 allele because they have the same number of functional copies of *ebony* as the reciprocal F₁ hybrids.
437

438 Consistent with a prior report (Bartelt et al. 1986), we found that *D. americana* and *D. novamexicana*
439 produced markedly different CHC profiles. Specifically, we found that CHCs with a chain length of
440 25 or fewer were only present in *D. novamexicana*, whereas CHCs with a chain length of 31 or
441 greater were only present in *D. americana* (Figure 5A). In both species, the loss of *ebony* function
442 had no qualitative effect on which CHCs were produced by either species, but increased the
443 abundance of some CHCs in both *D. americana* and *D. novamexicana* (Figure 5B,C). *ebony* loss-of-
444 function mutants in *D. melanogaster* were shown to preferentially increase the abundance of long
445 chain CHCs (Massey et al. X), and we observed a similar pattern in *D. americana* (Figure 5D). In *D.*
446 *novamexicana*, we observed the opposite pattern, however: CHCs with shorter chain lengths showed
447 greater increases in abundance in *ebony* null mutants (Figure 5E). The reason for this difference in
448 how *ebony* affects CHCs in *D. americana* and *D. novamexicana* remains unclear, but might have to
449 do with the different levels of *tan* expression in these two species (Cooley et al. 2012) given that *tan*
450 was also shown to affect CHC profiles in *D. melanogaster* (Massey et al. 2019b).
451

452 We also examined the CHC profiles of female F₁ hybrids produced by crossing *D. americana*

453 females with *D. novamexicana* males. We found that these F₁ hybrid females showed a CHC profile
454 that was distinct from both species, but more similar to *D. novamexicana* (Figure 6A): it contained
455 some of the short chain CHCs unique to *D. novamexicana* and none of the long chain CHCs unique
456 to *D. americana* (Figure 6A). As seen for both species, eliminating *ebony* function in F₁ hybrids by
457 making them homozygous for *ebony* null alleles caused an increase in abundance of some CHCs but
458 did not alter which CHCs were present (Figure 6B). Longer chain CHCs were more likely to show
459 increased abundance than shorter chain CHCs (Figure 6C), but this relationship was not as strong as
460 that seen for *D. americana* (Figure 5D). To determine whether divergence between the *D. americana*
461 and *D. novamexicana* *ebony* alleles affected CHCs profiles, we compared CHCs extracted from
462 females from the reciprocal hemizyosity test. These flies have only one functional *ebony* allele (*D.*
463 *americana* or *D. novamexicana*) in the F₁ hybrid genetic background. The CHC profiles from these
464 flies were not significantly different from each other (Figure 6D,E), indicating that allelic divergence
465 at *ebony* does not have a detectable effect on CHCs in this species pair.
466

467 5 Conclusions

468
469 Identifying the genes responsible for phenotypic differences between species remains a significant
470 challenge for evolutionary biology. This task is especially challenging when a gene contributing to
471 phenotypic divergence is located in a region of the genome inverted between species, which
472 precludes recombination-based mapping. Such is the case for the *ebony* gene in *D. americana* and *D.*
473 *novamexicana*. Prior work suggested that *ebony* might contribute to differences in overall body color
474 between these two species (Wittkopp et al. 2009; Cooley et al. 2012), but its location in an inversion
475 made it difficult to directly test this hypothesis. In this study, we overcame this hurdle by using
476 CRISPR/Cas9 genome editing to generate null mutants for *ebony* in *D. americana* and *D.*
477 *novamexicana*, and then using these mutants to perform a reciprocal hemizyosity test (Stern 2014),
478 which directly compares the effects of the two species' alleles on pigmentation. We found that
479 divergence at *ebony* does indeed contribute to differences in body color between *D. americana* and
480 *D. novamexicana*.

481
482 Characterizing the phenotypes of *D. americana* and *D. novamexicana* *ebony* mutants, as well as flies
483 from the reciprocal hemizyosity test, also identified effects of *ebony* on other phenotypes. For
484 example, we found that differences in the activity of *ebony* alleles between *D. americana* and *D.*
485 *novamexicana* are responsible for the absence of dark pigmentation seen along the dorsal abdominal
486 midline of *D. novamexicana* but not *D. americana*. This trait has previously been described as
487 derived in *D. novamexicana* (Spicer 1991); however, we see a similar dorsal midline lightening in at
488 least some lines of *D. lummei* (see Figure 1), another member of the virilis group, suggesting that the
489 dorsal midline activity of *ebony* existed prior to the divergence of *D. americana* and *D.*
490 *novamexicana*. An unexpected change in pupal pigment patterning was also seen in *D. americana*
491 and *D. novamexicana* *ebony* null mutants. Although *ebony* is known to affect pupal case
492 development in *D. melanogaster* (Sherald 1980), its loss causes a pale white pupa color rather than
493 the dark pigmentation we see in *D. americana* and *D. novamexicana* *ebony* null mutants. Because
494 *ebony* is required for the production of yellow pigments, the dark markings seen in *ebony* mutant
495 pupal cases likely result from expression of an enzyme required for synthesis of dark pigments, such
496 as *tan*. Finally, we found that *ebony* null mutants showed significant changes in the abundance of
497 some CHCs in each species, but divergence of *ebony* did not contribute to differences in the CHC
498 profiles seen between species. These observations illustrate how *cis*-regulatory changes can cause
499 divergence of some, but not all, traits affected by a pleiotropic gene.

500

501 Observations reported in this work were made possible by the ability to manipulate the *D. americana*
502 and *D. novamexicana* genomes with CRISPR/Cas9 genome editing. While this technology has great
503 potential for allowing functional hypothesis testing in species that have not historically been
504 considered genetic model systems, this work was not always straightforward. We hope that the
505 detailed descriptions of our genome editing efforts provided in the Materials and Methods section of
506 this paper will be helpful for other researchers striving to manipulate the genomes of non-model
507 species.
508

509 **6 Author Contributions**

510

511 AML and PJW conceived of the experiments. AML, PS, and ZW performed the experiments. HC
512 and PWJ provided funding, advice, and oversight. AML and PJW wrote the manuscript.
513

514 **7 Funding**

515

516 This work was funded by the National Institutes of Health (Grant No. 1R35GM118073 and Grant
517 No. 1R01GM089736) awarded to PJW; National Science Foundation Graduate Research Fellowship
518 Program (Grant No: DGC 1256260) and National Institute of Health training grant: "Michigan
519 Predoctoral Training in Genetics" (Grant No: T32GM00754) to AML; and startup funding provided
520 by Michigan State University AgbioResearch to HC.
521

522 **8 Conflict of Interest Statement**

523

524 The authors declare that the research was conducted in the absence of any commercial or financial
525 relationships that could be construed as a potential conflict of interest.
526

527 **9 Acknowledgements**

528

529 We thank Arnaud Martin (George Washington University) as well as Kathy Vaccarro and other
530 members of Sean Carroll's laboratory (University of Wisconsin) for advice on CRISPR/Cas9 genome
531 editing and *Drosophila* injections, respectively; Hannah McConnell, Aida de la Cruz, and Harmit
532 Malik (Fred Hutchinson Cancer Research Center) for sharing their experience working with the
533 *nanos* promoter in *Drosophila virilis*; and the Bloomington *Drosophila* Stock Center as well as the
534 National *Drosophila* Species Stock Center for maintaining and providing fly stocks
535

536 **10 References**

537

538 Ahmed-Braimah, Y.H. and McAllister, B.F. (2012). Rapid evolution of assortative fertilization
539 between recently allopatric species of *Drosophila*. *Int. J. Evol. Biol.* 2012, 285468. doi:
540 10.1155/2012/285468.

541

542 Ahmed-Braimah, Y.H. and Sweigart, A.L. (2015). A single gene causes an interspecific difference in
543 pigmentation in *Drosophila*. *Genetics* 200, 331–42. doi: 10.1534/genetics.115.174920.

543

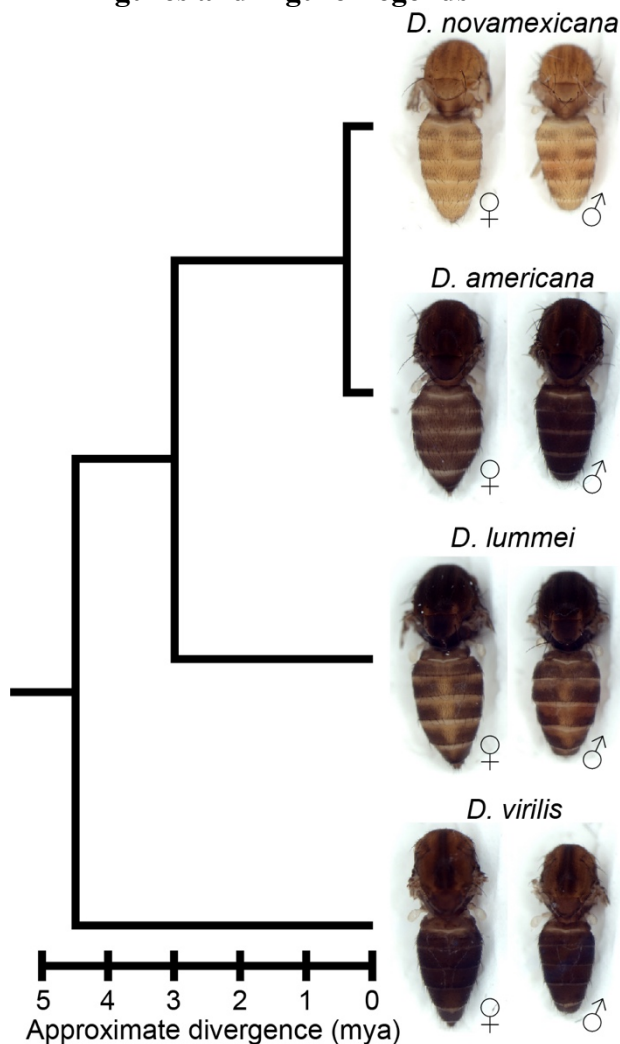
Bartelt, R.J., Arnold, M.T., Schaner, A.M., and Jackson, L.L. (1986). Comparative analysis of

- 544 cuticular hydrocarbons in the *Drosophila virilis* species group. *Comp. Biochem. Physiol. -- Part*
545 *B Biochem.* 83, 731–42. doi: 10.1016/0305-0491(86)90138-0.
- 546 Bassett, A.R., Tibbit, C., Ponting, C.P., and Liu, J.-L. (2013). Highly Efficient Targeted Mutagenesis
547 of *Drosophila* with the CRISPR/Cas9 System. *Cell Rep.* 4, 220–28. doi:
548 10.1016/j.celrep.2013.06.020.
- 549 Benjamini, Y. and Hochberg, Y. (1995). Controlling the false discovery rate : a practical and
550 powerful approach to multiple testing. *J. R. Stat. Soc. Ser. B* 57, 289–300.
551 <https://www.jstor.org/stable/2346101>.
- 552 Caletka, B.C. and McAllister, B.F. (2004). A genealogical view of chromosomal evolution and
553 species delimitation in the *Drosophila virilis* species subgroup. *Mol. Phylogenet. Evol.* 33, 664–
554 70. doi: 10.1016/j.ympev.2004.08.007.
- 555 Carroll, S.B. (2005). Evolution at two levels: on genes and form. *PLoS Biol.* 3, e245. doi:
556 10.1371/journal.pbio.0030245.
- 557 Chung, H. and Carroll, S.B. (2015). Wax, sex and the origin of species: Dual roles of insect cuticular
558 hydrocarbons in adaptation and mating. *BioEssays*, 822–30. doi: 10.1002/bies.201500014.
- 559 Chung, H., Loehlin, D.W., Dufour, H.D., Vaccarro, K., Millar, J.G., and Carroll, S.B. (2014). A
560 single gene affects both ecological divergence and mate choice in *Drosophila*. *Science* 343,
561 1148–51. doi: 10.1126/science.1249998.
- 562 Cooley, A.M., Shefner, L., McLaughlin, W.N., Stewart, E.E., and Wittkopp, P.J. (2012). The
563 ontogeny of color: developmental origins of divergent pigmentation in *Drosophila americana*
564 and *D. novamexicana*. *Evol. Dev.* 14, 317–25. doi: 10.1111/j.1525-142X.2012.00550.x.
- 565 Holtzman, S., Miller, D., Eisman, R., Kuwayama, H., Niimi, T., and Kaufman, T. (2010). Transgenic
566 tools for members of the genus *Drosophila* with sequenced genomes. *Fly (Austin)*. 4, 349–62.
567 doi: 10.4161/fly.4.4.13304.
- 568 Horn, C. and Wimmer, E.A. (2000). A versatile vector set for animal transgenesis. *Dev. Genes Evol.*
569 210, 630–37. doi: 10.1007/s004270000110.
- 570 Koch, P.B., Behnecke, B., Weigmann-Lenz, M., and Ffrench-Constant, R.H. (2000). Insect
571 pigmentation: Activities of β -alanyl-dopamine synthase in wing color patterns of wild-type and
572 melanic mutant swallowtail butterfly *Papilio glaucus*. *Pigment Cell Res.* 13, 54–58. doi:
573 10.1111/j.0893-5785.2000.130811.x.
- 574 Kronforst, M.R., Barsh, G.S., Kopp, A., Mallet, J., Monteiro, A., Mullen, S.P., Protas, M.,
575 Rosenblum, E.B., Schneider, C.J., and Hoekstra, H.E. (2012). Unraveling the thread of nature’s
576 tapestry: the genetics of diversity and convergence in animal pigmentation. *Pigment Cell*
577 *Melanoma Res.* 25, 411–33. doi: 10.1111/j.1755-148X.2012.01014.x.
- 578 Liu, M., Rehman, S., Tang, X., Gu, K., Fan, Q., Chen, D., and Ma, W. (2018). Methodologies for
579 Improving HDR Efficiency. *Front. Genet.* 9, 691. doi: 10.3389/fgene.2018.00691.
- 580 Massey, J. H. and Wittkopp, P.J. (2016). The genetic basis of pigmentation differences within and
581 between *Drosophila* species. In *Curr. Top. Dev. Biol.*, 119:27–61. doi:
582 10.1016/bs.ctdb.2016.03.004.
- 583 Massey, Jonathan H., Chung, D., Siwanowicz, I., Stern, D.L., and Wittkopp, P.J. (2019a). The *yellow*
584 gene influences *Drosophila* male mating success through sex comb melanization. *eLife* 8, 1–20.
585 doi: 10.7554/eLife.49388.
- 586 Massey, J. H., Akiyama, N., Bien, T., Dreisewerd, K., Wittkopp, P.J., Yew, J.Y., and Takahashi, A.
587 (2019b). Pleiotropic effects of *ebony* and *tan* on pigmentation and cuticular hydrocarbon
588 composition in *Drosophila melanogaster*. *Front. Physiol.* 10, 518. doi:
589 10.3389/fphys.2019.00518.
- 590 Miller, D.F.B., Holtzman, S.L., and Kaufman, T.C. (2002). Customized microinjection glass
591 capillary needles for P-element transformations in *Drosophila melanogaster*. *Biotechniques* 33,
592 366–75. doi: 10.2144/02332rr03.

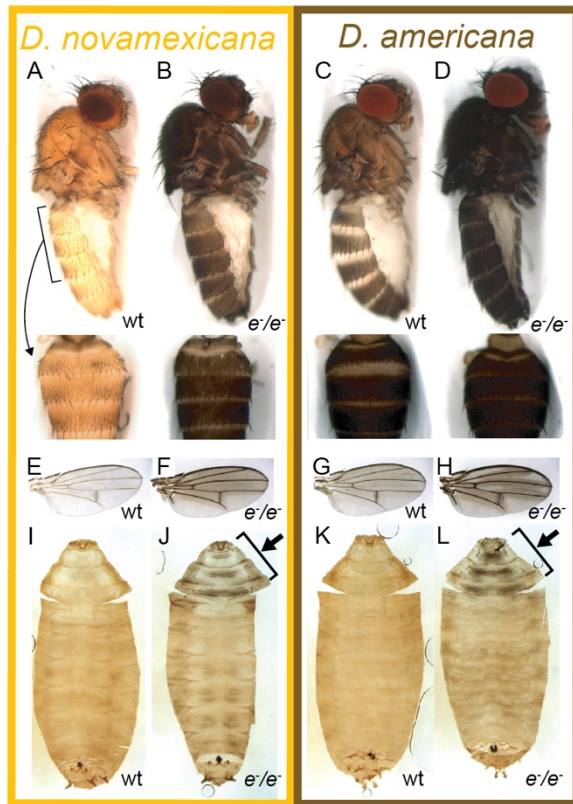
- 593 Morales-Hojas, R., Vieira, C.P., and Vieira, J. (2008). Inferring the evolutionary history of
594 *Drosophila americana* and *Drosophila novamexicana* using a multilocus approach and the
595 influence of chromosomal rearrangements in single gene analyses. *Mol. Ecol.* 17, 2910–26. doi:
596 10.1111/j.1365-294X.2008.03796.x.
- 597 Nappi, A.J. and Christensen, B.M. (2005). Melanogenesis and associated cytotoxic reactions:
598 Applications to insect innate immunity. *Insect Biochem. Mol. Biol.* 35, 443–59. doi:
599 10.1016/j.ibmb.2005.01.014.
- 600 Patterson, J.T. and Stone, W.S. (1949). The relationship of *novamexicana* to the other members of
601 the *virilis* group. In *Univ. Texas Publ.*, 4920:7–17.
- 602 Port, F., Chen, H.M., Lee, T., and Bullock, S.L. (2014). Optimized CRISPR/Cas tools for efficient
603 germline and somatic genome engineering in *Drosophila*. *Proc. Natl. Acad. Sci. U. S. A.* 111,
604 E2967-76. doi: 10.1073/pnas.1405500111.
- 605 Rebeiz, M. and Williams, T.M. (2017). Using *Drosophila* pigmentation traits to study the
606 mechanisms of cis-regulatory evolution. *Curr. Opin. Insect Sci.* 19, 1–7. doi:
607 10.1016/j.cois.2016.10.002.
- 608 Sherald, A.F. (1980). Sclerotization and coloration of the insect cuticle. *Experientia* 36, 143–46. doi:
609 10.1007/BF01953696.
- 610 Spicer, G.S. (1991). The genetic basis of a species-specific character in the *Drosophila virilis* species
611 group. *Genetics* 128, 331–37. <http://www.ncbi.nlm.nih.gov/pubmed/2071018>.
- 612 Stern, D.L. (2014). Identification of loci that cause phenotypic variation in diverse species with the
613 reciprocal hemizyosity test. *Trends Genet.* 30, 547–54. doi: 10.1016/j.tig.2014.09.006.
- 614 Stern, D.L., Crocker, J., Ding, Y., Frankel, N., Kappes, G., Kim, E., Kuzmickas, R., Lemire, A.,
615 Mast, J.D., and Picard, S. (2017). Genetic and transgenic reagents for *Drosophila simulans*, *D.*
616 *mauritiana*, *D. yakuba*, *D. santomea*, and *D. virilis*. *G3 (Bethesda)*. 7, 1339–47. doi:
617 10.1534/g3.116.038885.
- 618 Suh, J. and Jackson, F.R. (2007). *Drosophila ebony* activity is required in glia for the circadian
619 regulation of locomotor activity. *Neuron* 55, 435–47. doi: 10.1016/j.neuron.2007.06.038.
- 620 Takahashi, A. (2013). Pigmentation and behavior: potential association through pleiotropic genes in
621 *Drosophila*. *Genes Genet. Syst.* 88, 165–74. <http://www.ncbi.nlm.nih.gov/pubmed/24025245>.
- 622 Thurmond, J., Goodman, J.L., Strelets, V.B., Attrill, H., Gramates, L.S., Marygold, S.J., Matthews,
623 B.B., Millburn, G., Antonazzo, G., Trovisco, V., Kaufman, T.C., Calvi, B.R., and FlyBase
624 Consortium. (2019). FlyBase 2.0: the next generation. *Nucleic Acids Res.* 47, D759–65. doi:
625 10.1093/nar/gky1003.
- 626 True, J.R. (2003). Insect melanism: the molecules matter. *Trends Ecol. Evol.* 18, 640–47. doi:
627 10.1016/j.tree.2003.09.006.
- 628 True, J.R., Yeh, S.D., Hovemann, B.T., Kemme, T., Meinertzhagen, I. a, Edwards, T.N., Liou, S.R.,
629 Han, Q., and Li, J. (2005). *Drosophila tan* encodes a novel hydrolase required in pigmentation
630 and vision. *PLoS Genet.* 1, e63. doi: 10.1371/journal.pgen.0010063.
- 631 Wittkopp, P. J., Stewart, E.E., Arnold, L.L., Neidert, A.H., Haerum, B.K., Thompson, E.M., Akhras,
632 S., Smith-Winberry, G., and Shefner, L. (2009). Intraspecific polymorphism to interspecific
633 divergence: genetics of pigmentation in *Drosophila*. *Science*. 326, 540–44. doi:
634 10.1126/science.1176980.
- 635 Wittkopp, P J, Smith-Winberry, G., Arnold, L.L., Thompson, E.M., Cooley, a M., Yuan, D.C., Song,
636 Q., and McAllister, B.F. (2011). Local adaptation for body color in *Drosophila americana*.
637 *Heredity (Edinb)*. 106, 592–602. doi: 10.1038/hdy.2010.90.
- 638 Wittkopp, Patricia J, and Beldade, P. (2009). Development and evolution of insect pigmentation:
639 genetic mechanisms and the potential consequences of pleiotropy. *Semin. Cell Dev. Biol.* 20,
640 65–71. doi: 10.1016/j.semcdb.2008.10.002.
- 641 Wittkopp, Patricia J, Carroll, S.B., and Kopp, A. (2003). Evolution in black and white: genetic

- 642 control of pigment patterns in *Drosophila*. *Trends Genet.* 19, 495–504. doi: 10.1016/S0168-
643 9525(03)00194-X.
- 644 Wittkopp, Patricia J, True, J.R., and Carroll, S.B. (2002). Reciprocal functions of the *Drosophila*
645 yellow and ebony proteins in the development and evolution of pigment patterns. *Development*
646 129, 1849–58. <http://www.ncbi.nlm.nih.gov/pubmed/11934851>.
- 647 Wittkopp, Patricia J, Williams, B.L., Selegue, J.E., and Carroll, S.B. (2003). *Drosophila*
648 pigmentation evolution: divergent genotypes underlying convergent phenotypes. *Proc. Natl.*
649 *Acad. Sci. U. S. A.* 100, 1808–13. doi: 10.1073/pnas.0336368100.
- 650 Wray, G.A., Hahn, M.W., Abouheif, E., Balhoff, J.P., Pizer, M., Rockman, M. V, and Romano, L.A.
651 (2003). The evolution of transcriptional regulation in eukaryotes. *Mol. Biol. Evol.* 20, 1377–
652 1419. doi: 10.1093/molbev/msg140.
- 653

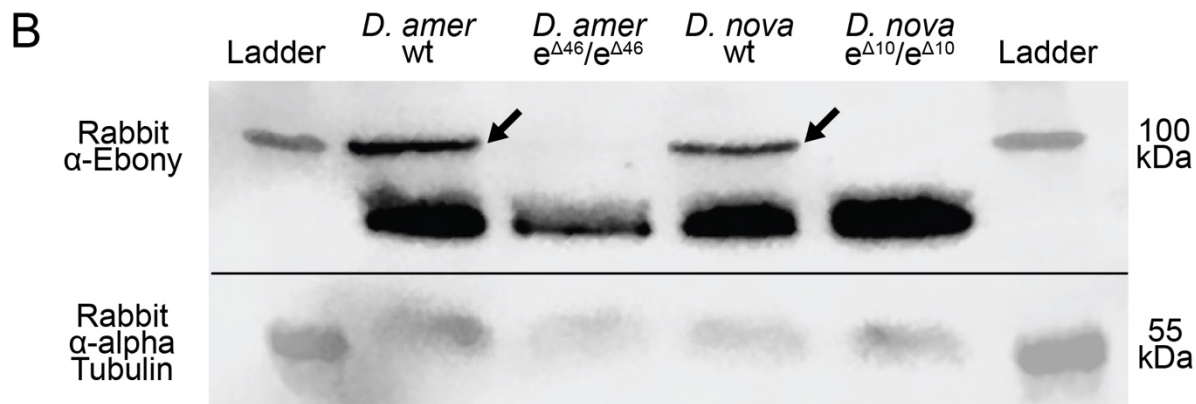
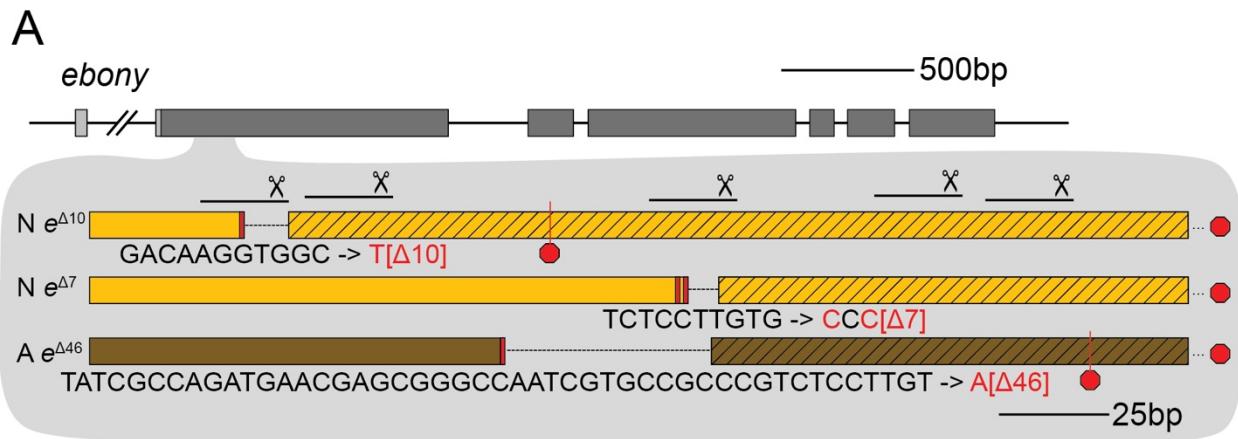
654 **11 Figures and Figure Legends**



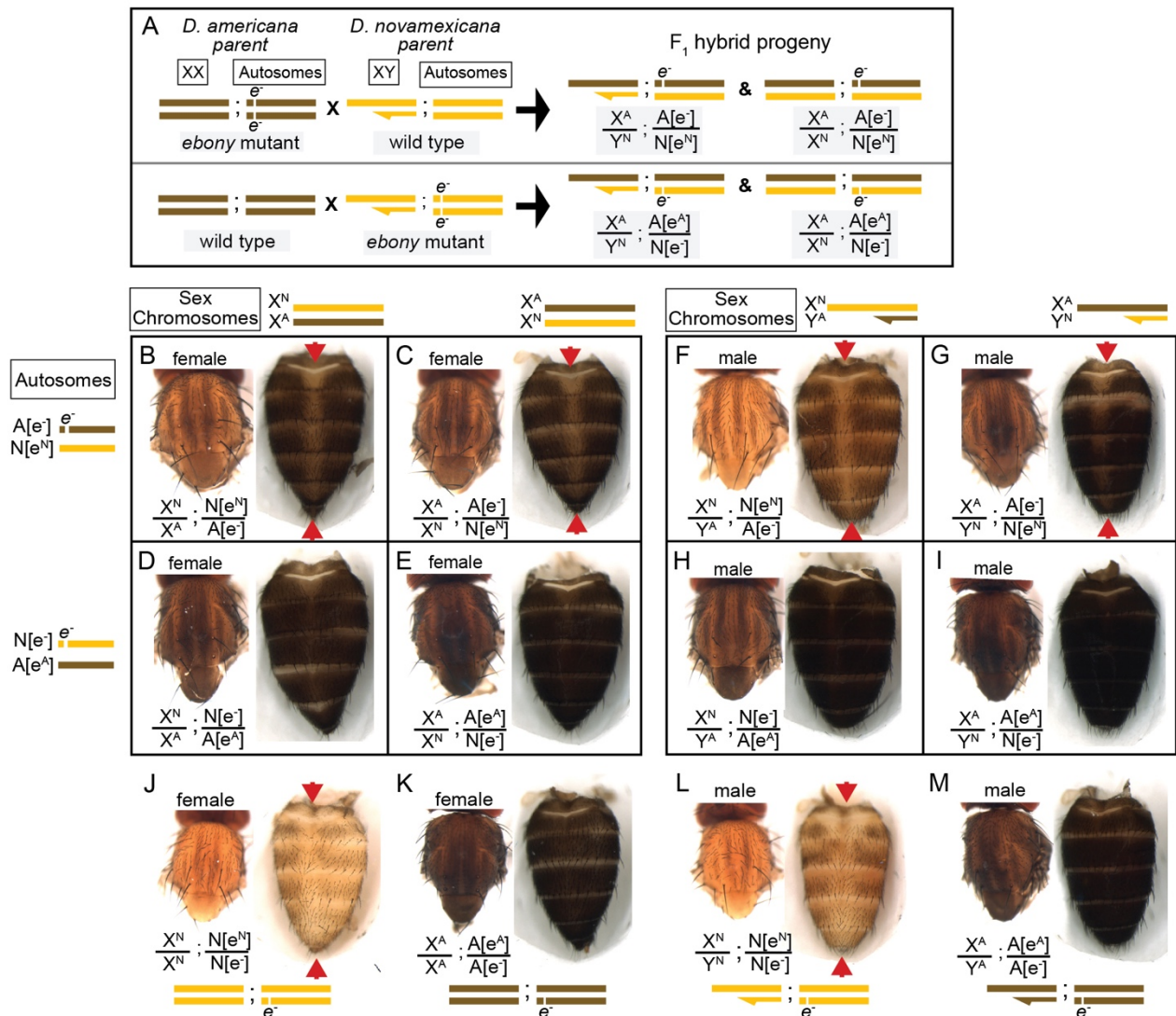
655 **Figure 1. *D. novamexicana* shows divergent body color within the virilis group.** Phylogenetic
656 relationships with estimated divergence times (Caletka and McAllister 2004; Cooley et al 2012) are
657 shown for *D. novamexicana*, *D. americana*, *D. lummei*, and *D. virilis*. For each species, a dorsal view
658 of the thorax and abdomen is shown for females (left) and males (right), with heads, wings, and legs
659 removed.
660
661



662
663 **Figure 2. Ebony affects body, wing, and pupal pigmentation in *D. novamexicana* and *D.***
664 ***americana*.** (A-D) Adult body pigmentation is shown from a lateral view (top) and dorsal abdominal
665 view (segments A2-A4, bottom) for (A) *D. novamexicana*, (B) *D. novamexicana* ebony null mutants,
666 (C) *D. americana*, and (D) *D. americana* ebony null mutants. (E-H) Adult wing pigmentation is
667 shown for (E) *D. novamexicana*, (F) *D. novamexicana* ebony null mutants, (G) *D. americana*, and
668 (H) *D. americana* ebony null mutants. (I-L) Pigmentation of pupal cases is shown for (I) *D.*
669 *novamexicana*, (J) *D. novamexicana* ebony null mutants, (K) *D. americana*, and (L) *D. americana*
670 *ebony* null mutants. Arrows in (J) and (L) highlight the most prominent areas with dark pigmentation
671 in *ebony* mutants.

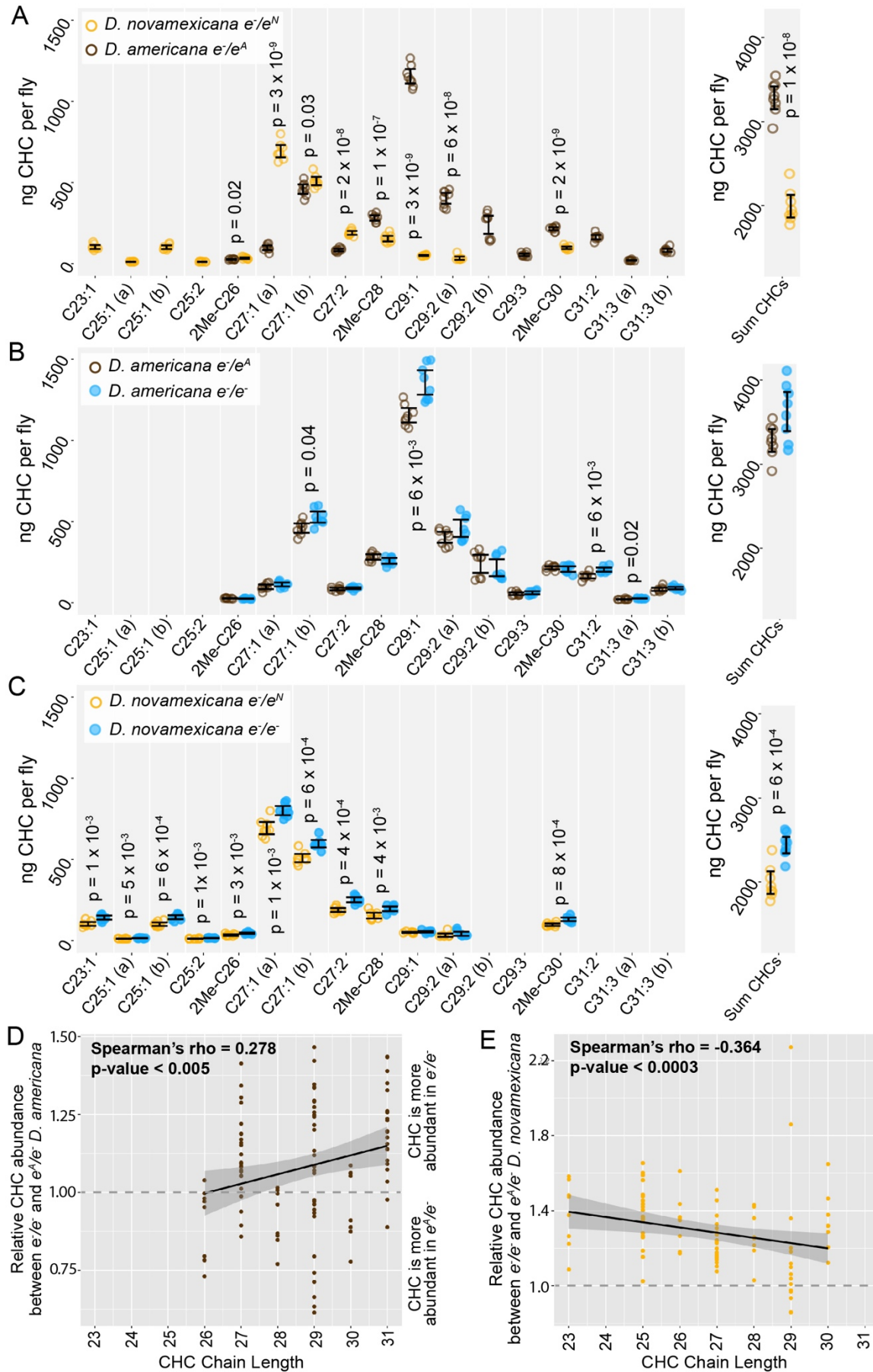


672
 673 **Figure 3. CRISPR/Cas9-induced mutations created null alleles of the *D. novamexicana* and *D.***
 674 ***americana* *ebony* genes. (A)** A schematic of the *ebony* gene is shown with grey boxes indicating
 675 exons; coding sequence is indicated in the darker shade of grey. Locations of the five guide RNAs
 676 targeting the second exon of *ebony* are shown with solid lines below scissor symbols. Mutations
 677 observed in the two *ebony* mutants ($e^{\Delta 10}$ and $e^{\Delta 7}$) isolated in *D. novamexicana* (“N”) and the one
 678 *ebony* mutant ($e^{\Delta 46}$) isolated in *D. americana* (“A”) are shown. All three alleles included deletions
 679 that caused frameshifts. (B) Western blotting showed that the *D. americana* $e^{\Delta 46}$ and *D.*
 680 *novamexicana* $e^{\Delta 10}$ mutants (lanes 2 and 4, respectively) lacked a ~100 kDa protein (arrows)
 681 recognized by an antibody raised against *D. melanogaster* Ebony protein (Wittkopp et al. 2002) that
 682 is present in wild-type (wt) *D. americana* and *D. novamexicana* (lanes 1 and 3, respectively).
 683 Relative abundance of total protein loaded into each lane can be seen by the relative intensities of the
 684 shorter proteins also detected by the Ebony antibody (Wittkopp et al. 2002) as well as the relative
 685 intensities of ~55kDa bands detected by an antibody recognizing alpha Tubulin (Abcam ab52866).
 686 The solid black line shows where the membrane was cut prior to incubation with primary antibodies
 687 during the western blotting procedure; the top half was incubated with anti-Ebony antibodies whereas
 688 the bottom half was incubated with anti-Tubulin antibodies. The two halves were realigned by hand
 689 for imaging, using the shape of the cut and the ladder staining as a guide. An un-annotated image of
 690 this blot is shown in Supplementary Figure 4.



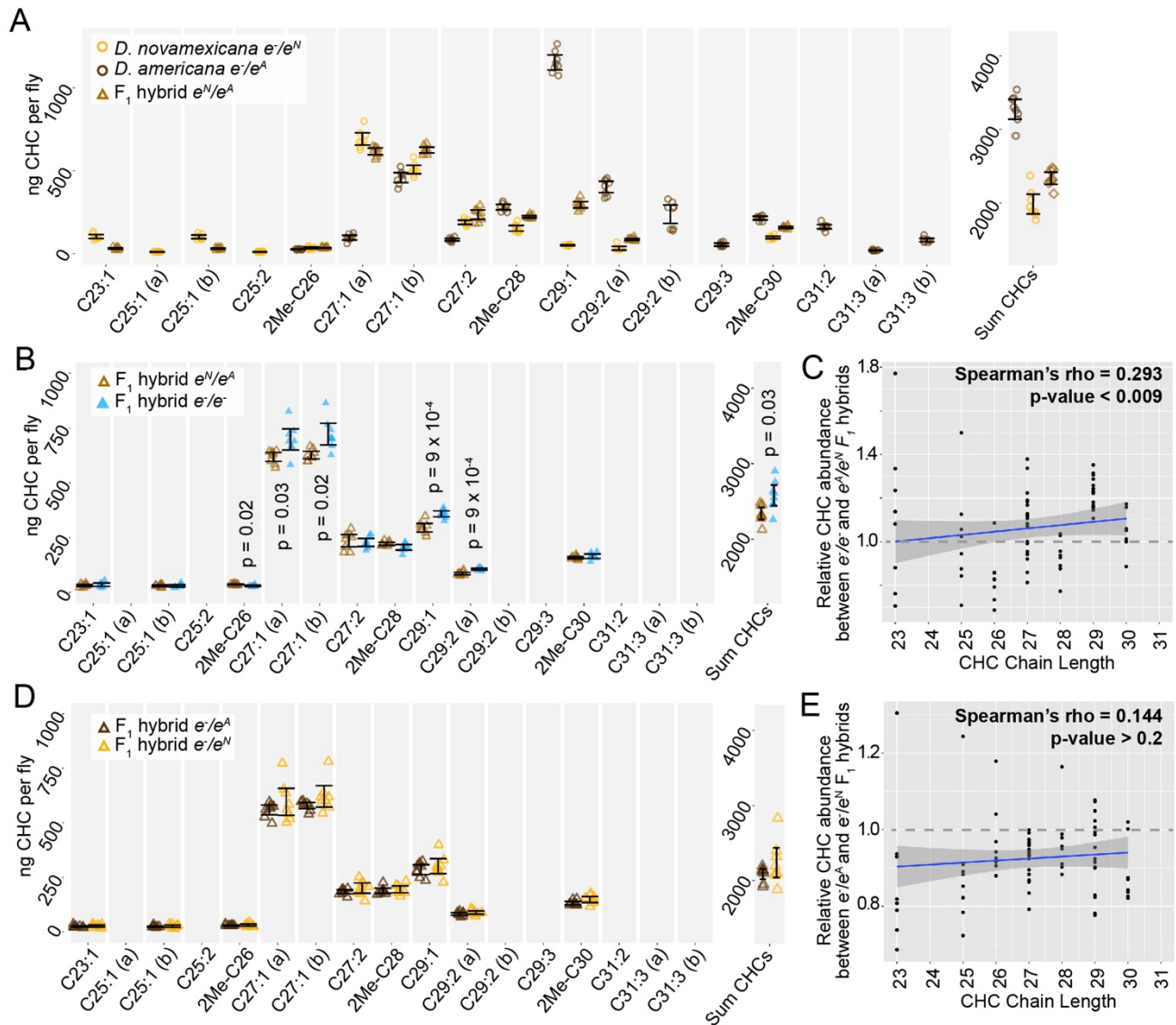
691
 692 **Figure 4. Reciprocal hemizyosity testing shows effects of *ebony* divergence between *D.***
 693 ***americana* and *D. novamexicana* on body pigmentation.** (A) Schematic shows representative sex
 694 chromosomes (XX and XY) and autosomes of the parents and progeny of reciprocal hemizyosity
 695 crosses, along with the genotypes of the progeny. Although a single autosome is shown for
 696 simplicity, these species have five autosomes. Superscript “A” and “N”, as well as brown and yellow
 697 colored bars, indicate alleles and chromosomes from *D. americana* and *D. novamexicana*,
 698 respectively; e^e indicates an *ebony* null allele. Although the schematic illustrates the crosses only with
 699 *D. americana* as the female parent, the same crosses were performed with sexes of the parental
 700 species reversed. (B–I) Dorsal thorax and abdomen phenotypes are shown for female (B–E) and male
 701 (F–I) progeny of reciprocal hemizyosity crosses. Genotypes of autosomal and sex chromosomes are
 702 shown to the left and above panels B–I, respectively, using the same schematic notation as in panel
 703 A. Individuals in B, C, F, and G carry a wild-type copy of *D. novamexicana* *ebony* allele, whereas
 704 individuals in panels D, E, H, and I carry a wild-type copy of the *D. americana* *ebony*. (J–M)
 705 Dorsal thorax and abdomen phenotypes are shown for female (J, K) and male (L, M) flies heterozygous
 706 for the *ebony* null allele in *D. novamexicana* (J, L) and *D. americana* (K, L) for comparison to flies
 707 shown in panels B–I, which also all carry one null and one wild-type *ebony* allele. Red arrowheads in

708 panels **B, C, F, G, J,** and **L** highlight the reduced dark pigmentation in the abdomen along the dorsal
709 midline relative to lateral regions.



711 **Figure 5. Cuticular hydrocarbons (CHCs) are affected by *ebony* and differ between *D. americana***
712 **and *D. novamexicana*.** (A-C) Abundance of individual CHC compounds (ng/fly) and summed CHCs
713 extracted from female flies are plotted for the following genotypes: (A) *D. americana* and *D.*
714 *novamexicana*, each heterozygous for an *ebony* null (*e*⁻) allele, (B) *D. americana* heterozygous and
715 homozygous for an *ebony* null allele, (C) *D. novamexicana* heterozygous and homozygous for an
716 *ebony* null allele. Eight biological replicates are shown for each genotype, with error bars
717 representing 95% confidence intervals. For each comparison, the p-value from a Welch's t-test with a
718 Benjamini-Hochberg multiple test correction ($\alpha = 0.05$) is shown when a significant difference in
719 abundance was detected for a CHC present in both genotypes being compared. CHCs are shown from
720 left to right with increasing chain length (represented by "C" followed by the chain length) with
721 double-bond and methyl-branched structures indicated by notations after the colon or before the "C",
722 respectively. For example, C25:1 represents a 25-carbon monoene, C25:2 represents a 25-carbon
723 diene, and 2Me-C28 represents a 28-carbon alkene with a methyl branch at the second carbon. (D-E)
724 Abundance of each CHC in *ebony* null mutants relative to flies heterozygous for the *ebony* null allele
725 is plotted by carbon chain length for (D) *D. americana* and (E) *D. novamexicana*. Black trendlines in
726 panels D-E show linear regressions, with shaded areas representing the standard error and both
727 Spearman's rho and p-values indicated on each plot.
728

729



730

731

732

733

734

735

736

737

738

739

740

741

742

743

744

745

746

Figure 6. *ebony* does not contribute to divergence of CHCs between *D. americana* and *D. novamexicana*. (A) Abundance of individual CHC compounds (ng/fly) and summed CHCs extracted from female flies are plotted for *D. americana* and *D. novamexicana* *ebony* heterozygotes as well as F_1 hybrids heterozygous for wild-type alleles of *ebony*. (B-C) CHCs from F_1 hybrids homozygous for *ebony* null alleles are compared to CHCs from F_1 hybrids with wild-type *D. americana* and *D. novamexicana* *ebony* alleles, showing the absolute abundance of individual and summed CHC compounds (B) as well as the relative abundance of CHCs by carbon chain length (C). In panel B, p-values are shown from a Welch's t-test with a Benjamini-Hochberg multiple test correction ($\alpha = 0.05$) when a significant difference in abundance was detected for a CHC present in both genotypes. (D-E) CHC profiles are plotted for reciprocal F_1 hybrids that differ only by which wild-type *ebony* allele they carry, either *D. americana* (e^A) or *D. novamexicana* (e^N), with absolute abundance of individual and summed CHCs shown in (D) and relative abundance of CHCs by chain length shown in (E). No p-values are shown in (D) because no CHCs showed a statistically significant difference in abundance between the two F_1 hybrid genotypes from the reciprocal hemizyosity test (Welch's t-test with Benjamini-Hochberg multiple test correction, $p > 0.05$ for each CHC). In panels C and E, blue trendlines show linear regressions, with shaded areas representing the standard error and both

747 Spearman's rho and p-values indicated on each plot. In all panels, data from eight replicate flies is
748 shown for each genotype.
749
750